Experimental and theoretical investigations of plasma oscillations of electrons in zinc and cadmium

V. D. Gorobchenko, M. V. Zharnikov, E. G. Maksimov, and S. N. Rashkeev

P. N. Lebedev Physics Institute, Academy of Sciences of the USSR, Moscow

(Submitted 26 July 1984)
Zh. Eksp. Teor. Fiz. **88**, 677–691 (February 1985)

The characteristic energy-loss spectra were measured for fast (30 keV) electrons penetrating right through thin Zn and Cd films. Although these metals belong to the same group in the periodic system, their spectra are strikingly different: in the case of Cd a narrow plasma-loss peak at 9.07 eV is typical of ordinary simple metals, whereas a plasma resonance exhibited by Zn begins from a threshold-type singularity near 9.3 eV and is followed by a wide peak at 14.3 eV. A theoretical analysis of the dielectric functions of Zn and Cd is carried out using the pseudopotential framework and also on the basis of the electron band structure of these metals calculated with allowance for the presence of narrow d bands. It is shown that the pseudopotential method describes correctly the width of the plasma resonance of Cd, but cannot account for the shift of the plasmon energy. In the case of Zn this approach is quite unsuitable. A calculation of the loss function carried out using a microscopic theory ensures a good agreement with the experimental data for Cd and predicts correctly the threshold nature of the onset of the plasma resonance of Zn. However, the overall agreement between the calculated and experimental spectra of Zn is only qualitative. The factors which might be responsible for the insufficient accuracy of theoretical calculations in the case of Zn are considered.

1. INTRODUCTION

Zinc and cadmium follow directly the noble metals copper and silver in the periodic system of elements and their ground-state atomic configurations are $[\mathrm{Ar}]3d^{10}4s^2$ and $[\mathrm{Kr}]4d^{10}5s^2$, respectively; they are polyvalent metals with the hexagonal close-packed (hcp) structure.

Experimental and theoretical investigations have established that near the Fermi surface of the conduction band both Zn and Cd are described quite satisfactorily by the model of almost-free electrons with a density of two electrons per atom. On this basis, both Zn and Cd are currently regarded as simple divalent metals with properties that depend weakly on the dynamics of the filled d bands and which satisfy ideally the necessary condition for the successful application of the pseudopotential formalism.[1] In this formalism the degrees of freedom of electrons of ionic cores are eliminated and an analysis is made of the problem of behavior of a gas of almost-free conduction electrons for which the effective periodic potential of the ions (i.e., the pseudopotential) is a weak perturbation. In the case of Zn and Cd there is a free electron gas with the parameters listed in Table I. Here, n_e is the density of conduction electrons, $r_s = (3/4\pi n_e)^{1/3}/a_B$, a_B is the Bohr radius, $E_F = \hbar^2(3\pi^2 n_e)^{2/3}/2m$ is the Fermi energy, and $\omega_p = (4\pi n_e e^2/m)^{1/2}$ is the classical frequency of plasma oscillations.

The correctness of the hypothesis that Zn and Cd are simple metals can be judged, for example, on the basis of the experiments involving excitation of plasma oscillations. The spectral distribution of the collective density of conduction electrons in simple metals can be described satisfactorily by a theory of Sturm (for a review see Ref. 2) and it is characterized by a strong resonance line located at a frequency close to ω_p. Attempts to determine the characteristics of a plasma resonance of conduction electrons in Zn and Cd have been made frequently over a period of more than three decades, but the net result of these investigations carried out by a variety of methods is very unsatisfactory because of the considerable discrepancies between the data obtained by different authors. This is made clear in Table II which lists the results of some of the most careful investigations. In this table the energy position of the plasma resonance is denoted by E_p and $\Delta E_{1/2}$ is the full width at half-maximum of this resonance. The abbreviation CEL is used for the characteristic energy losses observed when a sample is penetrated right through by an electron beam (the primary electron energy is given in parentheses). The observed scatter of the experimental results seems to us a direct evidence of the difficulty encountered in the preparation of thin-film Zn and Cd samples of sufficiently high quality. Although Table II contains some fairly similar values of E_p, neither these correlated results nor the other data on the plasma oscillation energies agree with the values of $\hbar\omega_p$ listed in Table I. This is unusual for simple metals and it shows that the nature of Zn and Cd is much more complex.

It would therefore be desirable to analyze thoroughly the role of the d electrons in these post-transition metals. According to Ref. 10, the results of x-ray photoelectron spectroscopy indicate that the binding energies of the $3d_{5/2}$

TABLE I.

	Zn	Cd
n_e, cm^{-3}	$1{,}315\cdot10^{23}$	$0{,}926\cdot10^{23}$
r_s	2,306	2,591
E_F, eV	9,428	7,467
$\hbar\omega_p$, eV	13,463	11,302

TABLE II.

Zn		Cd		Method, reference
E_p, eV	$\Delta E_{1/2}$, eV	E_p, eV	$\Delta E_{1/2}$, eV	
–	–	7,8	3	CEL (1.5 keV), Ref. 3
8,6	2,8	7,5	2,6	
17.0	5	15,1	4	CEL (1.5 keV), Ref. 4
Shoulder near 9.3 eV		9,1	1,2	Plasma radiation[5]
9,5	3,8	–	–	Optical reflection[6]
9,46	0,58	8,68	0,8	Photoemission[7]
Resonance not observed		9,4	0,8	CEL (40 keV), Ref. 8
17,8	–	19,2	–	Review monograph[9]

and $3d_{3/2}$ subbands in metallic zinc are 9.23 and 9.77 eV, whereas the binding energies of the $4d_{5/2}$ and $4d_{3/2}$ subbands in metallic cadmium are 10.20 and 11.15 eV, respectively. The same method was used in Ref. 11 to find the binding energies of the $4d$ subbands in metallic Cd and this gave similar values: 10.47 eV ($4d_{5/2}$) and 11.46 eV ($4d_{3/2}$). Therefore, in Zn and Cd there are relatively narrow d bands located at relatively small depths below the Fermi surface near the bottom of the conduction band, and in the case of Zn it is very likely that the $3d$ band intersects the conduction band. Investigations carried out on atomic vapors of Zn and Cd demonstrated[12] that the spin-orbit splitting of the d states in these elements is 0.37 eV (Zn) and 0.7 eV (Cd). These values are somewhat smaller than the corresponding splittings of the d bands in the metallic state, which indicates some "band" broadening of the d levels in metallic Zn and Cd. This raises the question of the validity of the classification of the d electrons in these metals as strongly bound (i.e., belonging to the individual ionic cores).

A direct confirmation of the collective nature of the $3d$ states in metallic Zn was obtained by Himpsel *et al.*,[13] who used the method of photoelectron spectroscopy with angular resolution to determine the dispersion curves for the $3d$ subbands in the [0001] direction (along the hexagonal axis) and who showed quite definitely that the higher of these subbands is characterized by a dispersion of 0.17 eV [the relevant critical points are separated from the Fermi energy by -9.60 eV (Γ_5^+) and -9.77 eV (Γ_6^+).] The results of Himpsel *et al.*[13] are in reasonable agreement with the results of theoretical calculations of the energy band structure of zinc reported in Refs. 14 and 15. According to these calculations the narrow $3d$ band of Zn should lie within the conduction band slightly above its bottom (located, as estimated by Juras *et al.*,[14] at 11 eV below the Fermi level), but already at energies slightly higher than the region occupied by the $3d$ states the electron band structure of this metal should assume the form typical of the model of almost-free electrons.

Since the excitation energies of the d electrons in Zn and Cd are close to $\hbar\omega_p$, both the d electrons and the s electrons exhibit a strong polarizability at frequencies of ω_p, which may give rise to interesting effects in the spectra of collective plasma oscillations of electrons in these metals.

In this situation we decided that it would be desirable to investigate experimentally once again in full detail the spectra of characteristic energy losses of electrons in metallic Zn and Cd. In addition, calculated the expected spectra in two variants: assuming that both Zn and Cd are simple metals, and also using the calculated energy band structures found with the s and d electrons taken into account simultaneously and on a par. The results are reported below.

2. SAMPLES AND EXPERIMENTAL RESULTS

Our experiments were carried out on a spectrometer designed to measure the energy distribution in an electron beam after it has crossed a thin film of the investigated substance. The spectrometer and its characteristics were described in detail in Refs. 16 and 17. The primary electron beam incident on the sample had an energy 30 keV; the elastic peak in the CEL spectra was well approximated by a Gaussian distribution with the rms deviation $\sigma = 0.275 \pm 0.005$ eV. The measurements were carried out at room temperature in the forward scattering regime.

One of the principal experimental difficulties was the preparation of high-quality thin Zn and Cd metal films. They were prepared by the method of thermal evaporation and deposition on a substrate kept at liquid nitrogen temperature. This procedure took place in 5×10^{-7} Torr vacuum using sufficiently pure (99.9%) initial metals, which were heated in tantalum helical evaporators. Initially the substrates were polished rock salt single crystals and glass plates with evaporated NaCl films. The investigated films were floated off these substrates in water and placed on a fine-mesh copper grid acting as the sample holder. However, this widely used method was unsuitable for Zn and Cd. The procedure of floating a sample in water resulted in considerable deterioration of the quality of the films which initially were characterized by a strong metallic luster, and the corresponding CEL spectra consisted of just broad resonance lines more characteristic of the oxide state of the investigated elements[18] than of their metallic phase.

Oxidation of the samples was avoided by constructing three-layer sandwiches in which the Zn or Cd film was central and protected on both sides by thin (50–100 Å) Al films. These sandwiches were evaporated in a vacuum chamber without exposure to the atmosphere. Plasma excitations in Al and Al_2O_3 have been thoroughly investigated (see, for example, Ref. 9) so that in principle we could separate from the background of these excitations the contribution made to the CEL spectrum by Zn or Cd. It was unexpectedly found, however, that when such a three-layer film was separated from the NaCl substrate it rolled into a tube and it could not be flattened without damaging the film. Therefore, we had to forgo the use of soluble NaCl substrates and prepared samples with a permanent substrate.

The latter was a thin collodion film which was deposited directly on a fine-mesh copper grid of the sample holder in accordance with the method described in Ref. 19. The CEL spectrum due to the collodion film (before the deposition of a metal film) is shown as the inset in Fig. 1. The first promising result obtained for a sample of the Al-Cd-Al-collodion type is shown in Fig. 1a. In addition to a strong elastic peak (from which the lost energy was reckoned), we observed clearly two narrow resonance lines located at energies of about 9 and 15 eV against the background of the continuous contribution by the collodion substrate. The second of these resonances had all the parameters corresponding to the excitation of plasmons in Al, so that we assumed that the peak at 9 eV was due to the energy losses as a result of creation of plasma excitations in metallic Cd.

This hypothesis was confirmed by the following experiments. A gradual reduction in the thickness of the protective Al coatings made it possible to prepare samples with the CEL spectra practically free of the resonance line at 15 eV. A spectrum of this kind is shown in Fig. 1b for Cd. The dominant feature of this spectrum is a strong and narrow plasma resonance at 9 eV standing out clearly from the background due to the contribution of the collodion substrate (and that due to thin protective Al_2O_3 films with the CEL spectra approximately of the same kind as that of collodion). A weak resonance line near ~6 eV is most probably due to the excitation of surface plasmons. In the case of a Zn multilayer sample prepared by a similar technology we obtained the spectrum shown in Fig. 1c, quite different from that observed for Cd. In the case of Zn the strongest feature in the CEL spectrum is a threshold near 9.3 eV. As we pass through this threshold, the absorption intensity rises steeply within an energy interval less than 1 eV and this is followed by a small plateau and then by a relatively weak and broad resonance line centered at ~14.3 eV.

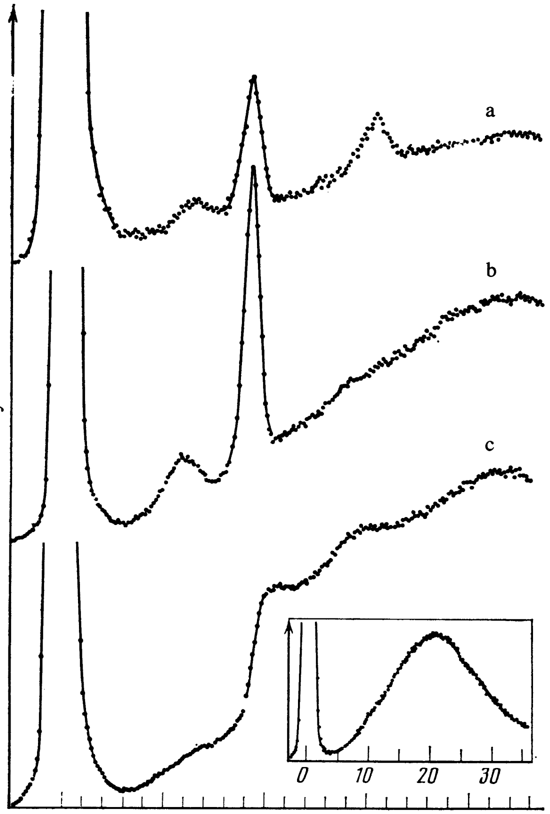

FIG. 1. Characteristic energy loss spectra of three-layer sandwiches deposited on a thin collodion film: a), b) Al-Cd-Al; c) Al-Zn-Al. In the last two cases, (b, c) the thickness of the protective film is selected so that the resonance line of Al at 15 eV is effectively suppressed. The inset shows the characteristic energy loss spectrum of the collodion substrate before the deposition of a metal film.

Selection of the evaporation conditions enabled us to dispense with a protective aluminum film and deposit directly (on collodion substrates) films of Zn and Cd of sufficiently high quality and about 500–600 Å thick in which the metallic layer predominated over the oxide film on the surface. This was confirmed by suitable electron photomicrographs and electron-diffraction patterns. According to the results, the grain size in the Cd films varied within the range ~700–1900 Å, whereas in the Zn films it was within the range ~300–750 Å. The electron-diffraction pattern of Zn exhibited a weak diffraction ring which could be attributed to zinc oxide. There was no clear indication of the presence of an oxide film on Cd in the electron diffraction pattern of the latter. The CEL spectra recorded for these samples are shown in Fig. 2. We can easily see that all the characteristic features of the spectra obtained earlier for samples with aluminum protective coatings (Fig. 1) appeared also in the spectra of Fig. 2, but even more clearly. The spectrum of Cd exhibited a clear peak of double plasma losses at the energy of 18.15 eV, which was practically absent from the spectrum of a thinner Cd film in a sandwich.

An analysis of nine CEL spectra of Cd carried out for the main plasma resonance gave the parameters

$$E_p=9{,}07\pm0{,}01\ \text{eV},\quad \Delta E_{1/2}=0{,}89\pm0{,}02\ \text{eV}, \tag{1}$$

where $\Delta E_{1/2}$ is the total observed width of the plasma peak at its half-amplitude, uncorrected for the finite energy resolution of the measuring apparatus. The values given in Eq. (1) are in satisfactory agreement with the corresponding parameters listed in Refs. 5, 7, and 8. If we ignore the fact that the value of E_p is strongly shifted downward relative to the initial plasmon energy $\hbar\omega_p = 11.3$ eV (Table I), we can say that (taken as a whole) the plasma resonance of electrons in Cd is still very characteristic of the family of simple metals and, moreover, it is one of the narrowest resonances of this type.

As for the plasma resonance of Zn, it is outwardly very different from the simple single peak exhibited by Cd (and resembles a shoulder also reported in Ref. 5). It should be pointed out that the steep rise of the energy losses in the region of 9–10 eV observed in the Zn spectrum is practically discontinuous (threshold). This follows from the observation that differentiation of this part of the spectrum gives a peak of approximately Gaussian profile located at $E_d = 9.30 \pm 0.05$ eV with an rms deviation $\sigma = 0.28 \pm 0.01$ eV, i.e., it

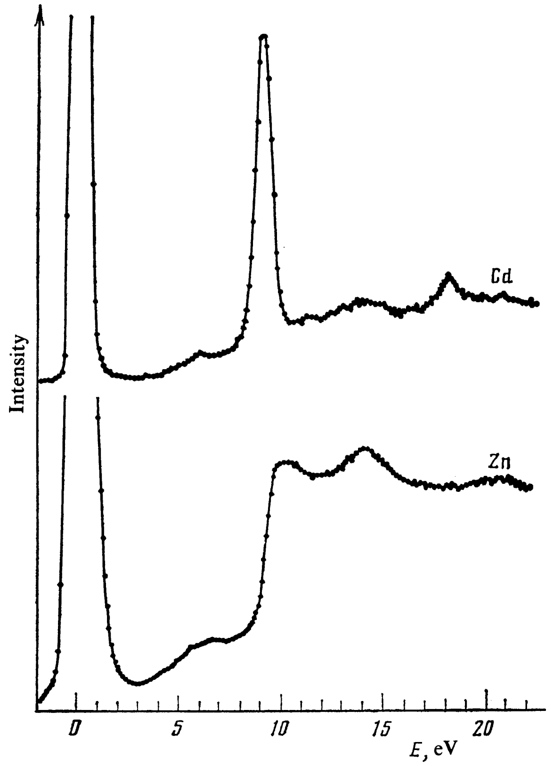

FIG. 2. Characteristic energy loss spectra of Cd and Zn samples deposited on collodion substrates.

is practically as narrow as the elastic scattering peak. Another feature of the CEL spectrum of Zn is the presence of a relatively wide but nevertheless strongly pronounced resonance peak at $E_p = 14.30 \pm 0.05$ eV, which is only slightly higher than the energy $\hbar\omega_p = 13.5$ eV of the corresponding "bare" plasmon. The first of these features has been tentatively recorded by other methods in Refs. 5, 6, and 7, whereas the second feature has not been observed before.

A more detailed discussion of the results obtained and of their possible physical meaning is given in the next section.

3. THEORETICAL ANALYSIS OF THE RESULTS

Interpretation of the spectra of the inelastic scattering of fast electrons in a solid is based on theoretical ideas on its permittivity; the latter governs the collective response of the charged interacting particles of the investigated substance to introduction of an external charge. A considerable contribution to the cross section of such scattering in metals is made by conduction electrons, in which a plasma resonance may be excited in the form of high-frequency collective oscillations of the electron density. These oscillations involve the passive participation of the discrete lattice formed by the positive low-mobility ion cores, which taken together exert a restoring force to the electron subsystem.

In the simplest theoretical model of a metal its conduction electrons are regarded as a homogeneous gas of charged fermions, which move against the background of a uniformly distributed (over the bulk of the metal) total positive ion charge. The spectrum of the CEL of such a hypothetical system is described in terms of the loss function

$$L(\mathbf{q}, \omega) = \mathrm{Im}\,[-1/\varepsilon(\mathbf{q}, \omega)], \tag{2}$$

where $\hbar\omega$ and $\hbar\mathbf{q}$ are the energy and momentum transferred to the system by a scattering event; $\varepsilon(\mathbf{q}, \omega)$ is its dielectric function and depends on the wave vector and on frequency (see, for example, the review[20]). A plasma resonance in the CEL spectrum corresponds to a pole of the loss function (2), located at $\mathbf{q} = 0$ at the classical plasma oscillation frequency ω_p. The general features of the characteristic losses predicted by Eq. (2) are exhibited by simple metals in which the conduction-electron subsystem approaches closest a homogeneous electron gas. However, even in these simplest objects many details of the CEL spectra can only be explained if we allow for the intraction between electrons and the crystal potential.

The presence of the periodic potential of the ions has the effect that one-electron states are no longer plane waves but are described by Bloch functions. This results in qualitative changes in the dielectric properties of the electron subsystem. These changes are manifested primarily by the fact that instead of one dielectric function $\varepsilon(\mathbf{q}, \omega)$, we now have a dielectric matrix

$$\varepsilon(\mathbf{k}+\mathbf{G}, \mathbf{k}+\mathbf{G}', \omega) \equiv \hat{\varepsilon}_{\mathbf{G}\mathbf{G}'}(\mathbf{k}, \omega), \tag{3}$$

which is defined in the space, of macroscopically large dimensionality, of the vectors of a reciprocal lattice $\{\mathbf{G}\}$. Here and later $\mathbf{k}$ is the wave vector within the first Brillouin zone. (The properties of the dielectric matrix of Bloch electrons are considered in Ref. 21 with allowance for the exchange-correlation effects.) More difficult to describe is the CEL spectrum of a crystalline substance, which is now described by a loss function of the type

$$L(\mathbf{q}, \omega) = -\mathrm{Im}\,\hat{\varepsilon}_{\mathbf{G}\mathbf{G}}^{-1}(\mathbf{k}, \omega), \tag{4}$$

where $\mathbf{q} = \mathbf{k} + \mathbf{G}$, and which contains a corresponding diagonal element of a matrix that is the inverse of Eq. (3). When the electron band structure of a metal is known, calculation of its dielectric matrix meets with no fundamental difficulties, at least in the most frequently used random-phase approximation,[22–24] although in practice it represents a time-consuming numerical problem. The subsequent inversion of the dielectric matrix needed to find the response function (4) has no general solution (in particular, there is no such solution for transition metals).

In the case of simple metals when the pseudopotential of the electron-ion interaction is weak and the nondiagonal elements of the dielectric matrix are correspondingly small, inversion of this matrix can be performed analytically by perturbation theory. The relevant theoretical treatment based on the random-phase approximation was developed in detail by Sturm and it has been confirmed by a number of experiments (for a review see Ref. 2). To within terms of the second order in the electron-ion pseudopotential, Sturm's theory gives the following expression for the loss function (4) in the case of interest to us when the transferred momentum $\mathbf{q} \to 0$

$$L(\omega) = \lim_{\mathbf{k} \to 0} \left[\frac{\varepsilon_2(\mathbf{k}, \omega)}{\varepsilon_1^2(\mathbf{k}, \omega) + \varepsilon_2^2(\mathbf{k}, \omega)} \right], \tag{5}$$

where $\varepsilon_1(\mathbf{k}, \omega)$ and $\varepsilon_2(\mathbf{k}, \omega)$ are the real and imaginary parts of the macroscopic dielectric function $\varepsilon_M(\mathbf{k}, \omega)$, which in the case of small values of $\mathbf{k}$ is given by

$$\varepsilon_M(\mathbf{k}, \omega) \approx 1 - \frac{\omega_p^2}{\omega^2} - \frac{1}{m^2\omega^4} \times \sum_{\mathbf{G} \neq 0} \left(\frac{\mathbf{kG}}{kG} \right)^2 |G^2 V_L(\mathbf{G})|^2 \left[\frac{1}{\varepsilon(\mathbf{G}, \omega)} - \frac{1}{\varepsilon(\mathbf{G}, 0)} \right]. \tag{6}$$

Here, $\varepsilon(\mathbf{G}, \omega)$ is the dielectric function of a homogeneous electron gas of appropriate density and $V_L(\mathbf{G})$ is the Fourier component of the lattice potential and can be represented in the form

$$V_L(\mathbf{G}) = N_a V(\mathbf{G}) S(\mathbf{G}), \tag{7}$$

where N_a is the total number of atoms, $V(\mathbf{G})$ is the form factor of the pseudopotential of the electron-ion interaction, and

$$S(\mathbf{G}) = \frac{1}{\nu} \sum_{s=1}^{\nu} e^{-i\mathbf{G}\boldsymbol{\rho}_s}$$

is the structure factor ($\boldsymbol{\rho}_s$ is the radius vector of the sth atom and ν is the total number of atoms in a unit cell).

We calculated the macroscopic dielectric function (6) and the loss function (5) for the cases of Cd and Zn using the local Heine-Abarenkov model potential:

$$V(\mathbf{r}) = \begin{cases} \dfrac{Ze^2}{r_0} u, & r \leqslant r_0 \\ -Ze^2/r, & r > r_0 \end{cases} \tag{8}$$

and using the dielectric function of a homogeneous electron gas considered in the random phase approximation. The value of Z was taken to be 2 and the parameters r_0 and u were assumed to be the same as in Ref. 25, where a calculation of the phonon spectra of Zn and Cd was reported. The Fourier component of the model potential (8) was used as the form factor $V(\mathbf{G})$ in the lattice potential (7). It should be pointed out that although the function (6) considered in the long-wavelength limit is independent of the absolute value of the wave vector $\mathbf{k}$, in the case of the hcp lattice it is anisotropic, namely it depends on the orientation of the vector $\mathbf{k}$ relative to the hexagonal symmetry axis c. For each fixed angle θ between the vector $\mathbf{k}$ and the c axis the curve representing the loss function (5) is a resonance peak with a nearly Lorentzian profile and its position as well as the total width at half-amplitude depend on the angle θ in accordance with the formulas

$$E_p = \hbar\omega_p - (\Delta_\parallel \cos^2\theta + \Delta_\perp \sin^2\theta),$$
$$\Delta E_{1/2} = \Gamma_\parallel \cos^2\theta + \Gamma_\perp \sin^2\theta. \tag{9}$$

The calculated values of the parameters Δ and Γ, which determine the shift of a plasma resonance relative to the "bare" plasmon energy $\hbar\omega_p$, and its width are listed in Table III (all the values in this table are in electron volts). In the case of polycrystalline samples, which were investigated by us, we are interested in the loss function averged over the spatial orientations of the vector $\mathbf{k}$. It is clear from Eq. (9) and Table III that the anisotropy of the resonance parameters predicted theoretically for Cd and Zn is weak so that the plasma loss peaks of polycrystalline samples of these metals should not be broadened too much. The broadening can be reproduced analytically. The resultant loss functions then assume the form shown in Fig. 3 and they are in the form of narrow resonance peaks.

A comparison of Figs. 2 and 3 demonstrates above all that the profile of the observed CEL spectrum of Zn cannot be described even approximately by Sturm's theory. In the case of Cd the experimental results do correspond to the theoretical predictions.

Thus, the pseudopotential approach to the electron band structure accounts satisfactorily for the width of the plasma resonance observed in Cd and estimated by us to be 0.44 ± 0.03 eV [this is the width of the Lorentzian curve which, on convolution with a Gaussian distribution characterized by $\sigma = 0.275 \pm 0.005$ eV, transform into a resonance peak with the experimentally observed given in Eq. (1)]. This accounts for the main channel of plasmon decay in Cd, namely creation of electron-hole pairs in the conduction band involving umklapp processes (in a homogeneous electron gas with $k \approx 0$ such a decay is forbidden by the laws of conservation of energy and momentum).

The pseudopotential approach predicts for Cd a plasma-resonance shift due to the additional polarizability which an electron gas acquires in the presence of electron-ion interaction, but this shift is almost an order of magnitude less than the experimental value. Hence, we may assume that in the case of Cd the reduction in the plasma oscillation energy from $\hbar\omega_p = 11.3$ eV to $E_p = 9.07$ eV is mainly due to the polarizability of the $4d$ electrons. This effect has been discussed qualitatively on many occasions (see, for example, Refs. 2 and 17). In particular, a renormalization of the plasmon energy to lower values shows that the $4d$ band of Cd should (in full agreement with the results of Refs. 10 and 11) be separated from the Fermi level by more than 9.07 eV. However, a quantitative description of this effect requires a microscopic calculation of the contribution of the $4d$ electrons to the dielectric matrix (3) and a subsequent accurate

TABLE III.

	$\Delta_\parallel$	$\Delta_\perp$	$\Gamma_\parallel$	$\Gamma_\perp$
Cd	0,316	0,159	0,478	0,687
Zn	0,106	0,007	0,310	0,475

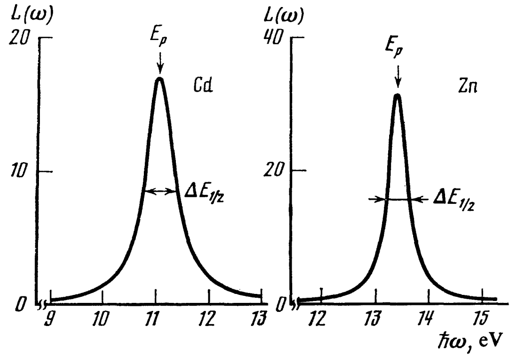

FIG. 3. Loss functions of polycrystalline Cd and Zn samples, calculated from Eq. (6) using the local Heine-Abarenkov potential of Eq. (8).

calculation of the loss function (4). As pointed out above, this is a very difficult task, so that we carried out some simplified calculations both for Cd and Zn, allowing nonetheless for the contribution of the d electrons. The results will be given below after a preliminary qualitative analysis of the CEL spectrum observed in the case of Zn.

Allowing for the threshold nature of the singularity observed at $E_d = 9.3$ eV in the spectrum of Zn, it is natural to assume that in the vicinity of this energy an interband absorption mechanism begins to act and excites the $3d$ electrons to vacant states above the Fermi surface. We can estimate qualitatively the influence of such interband transitions on the behavior of collective electron oscillations by employing the simplest expression for the frequency-dependent dielectric function:

$$\varepsilon(\omega)=1-\frac{f_0\omega_p^2}{\omega(\omega+i\gamma_0)}+\varepsilon_d(\omega), \tag{10}$$

where

$$\varepsilon_d(\omega)=-\sum_j\frac{f_j\omega_p^2}{\omega^2-\omega_j^2+i\gamma_j\omega}. \tag{11}$$

The first two terms in Eq. (10) represent the usual Drude-Lorentz expression for the intraband contribution to $\varepsilon(\omega)$, in which f_0 and γ_0 are, respectively, the oscillator strength and the reciprocal of the relaxation time for electron states near the Fermi surface. The additional term $\varepsilon_d(\omega)$, given by the classical expression (11), descibes the contribution made by the interband transitions with frequencies ω_j, oscillator strengths f_j, and widths γ_j. In the case of interest to us the value of ω_j varies continuously from $E_1(\approx E_d)$ to ∞, so that in Eq. (11) we can go over from summation in respect of j to integration with respect to ω_j. We can then assume that the oscillator strengths f_j decrease on increase in ω_j in accordance with the relation $f_j \propto 1/\omega_j^2$, and assume also that $\gamma_j = \text{const} = \gamma_1$. Consequently, the contribution (11) becomes

$$\begin{aligned}\varepsilon_d(\omega)&=f_1\omega_p^2E_1^2\int_{E_1}^{\infty}\frac{d\varepsilon}{\varepsilon^3(\varepsilon^2-\omega^2-i\gamma_1\omega)}\\&=\frac{f_1\omega_p^2}{2\omega(\omega+i\gamma_1)}\left[\frac{E_1^2}{\omega(\omega+i\gamma_1)}\ln\left(\frac{E_1^2}{E_1^2-\omega^2-i\gamma_1\omega}\right)-1\right].\end{aligned} \tag{12}$$

It should be pointed out that in the case of sufficiently small damping γ_1 the real part of the function (12) has a sharp peak at $\omega \approx E_1$, whereas the imaginary part has a steep step.

Figure 4 shows the loss function $L(\omega)$ calculated using the model dielectric function of Eqs. (10) and (12) for the set of parameters listed in the caption of this figure. It is clear from Fig. 4 that the calculated curve $L(\omega)$ is a fairly unusual resonance consisting of a wide line centered at an energy $\sim\hbar\omega_p$ and a very sharp peak in the left wing of this line near the energy E_1. The steep rise of this peak in a narrow range of energies to the left of the interband absorption edge is due to the rapid approach of the real part of $\varepsilon_1(\omega)$ to the abscissa when the values of the imaginary part $\varepsilon_2(\omega)$ are still small (the behavior of these functions is shown in Fig. 4 by chain and dashed curves, respectively). The slope of the right-hand side of the narrow peak is governed by a complex interplay between the functions $\varepsilon_1(\omega)$ and $\varepsilon_2(\omega)$.

The calculated loss function can be compared with the observed spectrum by convolution of $L(\omega)$ with the instrumental resolution function. Near the threshold energy E_1 there is a steep rise of the potential, whereas the wide peak is not greatly affected. We must remember that at energies slightly higher than E_1 the $3d$ band of Zn is split by the crystal-field and spin-orbit interaction effects, so that we cannot expect an exact reproduction of the form of the spectrum in this range of energies without appropriate precise calculations. However, since the width of the $3d$ band of Zn does not exceed 1 eV, it is clear that on the whole a plasma resonance of electrons in this metal is of two-humped nature, like the $L(\omega)$ curve of Fig. 4, and this is indeed observed experimentally.

We were able to provide a more realistic interpretation of the CEL spectra of Cd and Zn by microscopic calculations of the loss function (5) starting from the expression for the permittivity of a crystal considered in the self-consistent

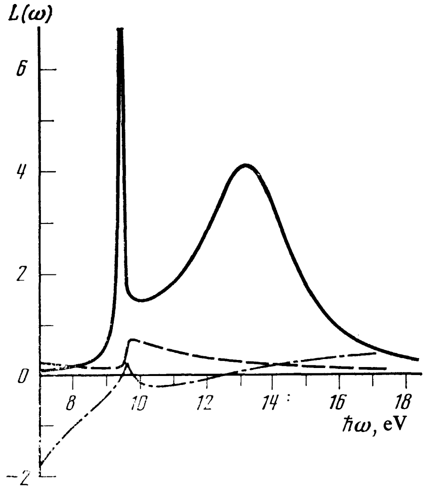

FIG. 4. Loss function $L(\omega)$ of Zn calculated using the model dielectric function of Eqs. (10) and (12) with the following set of parameters: $\omega_p = 13.5$ eV, $\gamma_0 = 0.5$ eV, $f_0 = 0.8$, $E_1 = 9.6$ eV, $\gamma_1 = 0.1$ eV, $f_1 = 0.25$. The dashed and dash-dot curves represent respectively the imaginary and real parts of the dielectric function of Eqs. (10) and (12).

field approximation[26]:

$$\varepsilon(\mathbf{q},\omega)=1-2v(\mathbf{q})\sum_{\lambda\lambda'\mathbf{k}}\frac{f_{\lambda\mathbf{k}}-f_{\lambda'\mathbf{k}+\mathbf{q}}}{\hbar\omega-E_{\lambda'\mathbf{k}+\mathbf{q}}+E_{\lambda\mathbf{k}}+i\delta}\times|\langle\lambda'\mathbf{k}+\mathbf{q}|e^{i\mathbf{q}\mathbf{r}}|\lambda\mathbf{k}\rangle|^2, \qquad (13)$$

where $|\lambda\mathbf{k}\rangle$ is a Bloch state with a band index λ and a quasiwave vector $\mathbf{k}$, which corresponds to the energy $E_{\lambda\mathbf{k}}$; $f_{\lambda\mathbf{k}}$ is the Fermi occupancy function of one-electron states; $v(\mathbf{q})$ is the Fourier component of the Coulomb potential.

The energy band structures of Cd and Zn were calculated by the LMTO (linear muffin-tin orbital) method developed by Andersen.[27] We used the self-consistent crystal potentials given in the book by Moruzzi *et al.*,[15] but we modified somewhat the constants of the exchange-correlation contributions in order to ensure coincidence of the centers of the d bands with the experimental positions. (A similar procedure was used in Ref. 13 to reproduce successfully the spectrum of the $3d$ band of Zn in good agreement with the experimental data of the authors.) We simplified the calculations by replacing the real hcp structures of Cd and Zn with the more symmetric fcc structures. This replacement was not very important in the calculation of many characteristics of metals associated with the d electrons because in both hcp and fcc structures the atoms have the same number of the nearest neighbors right up to the third coordination sphere. The satisfactory results obtained on replacement of the hcp with the fcc lattice in calculations of the energy band structure were demonstrated in Ref. 13.

We used the energy band structure to calculate directly the imaginary part of the interband ($\lambda\neq\lambda'$) contribution to the dielectric function (13) in the long-wavelength limit $q=0$ and then we found the corresponding real part from the dispersion relationship

$$\varepsilon_1(\omega)=1+\frac{2}{\pi}\int_0^\infty d\omega'\frac{\omega'\varepsilon_2(\omega')}{\omega'^2-\omega^2}. \qquad (14)$$

In the case of the intraband ($\lambda=\lambda'$) contribution to the dielectric function of Eq. (13) at $q=0$ we used the Drude-Lorentz formula [first two terms in Eq. (10)]. An explicit expression for the quantity $\tilde\omega_p^2=f_0\omega_p^2$ deduced from Eq. (13) can be found in Ref. 17. The detailed procedure used in the calculation of the energy band structure and the values of $\varepsilon_2(\omega)$ and $\tilde\omega_p^2$ were taken from Ref. 28.

The functions $\varepsilon_1(\omega)$, $\varepsilon_2(\omega)$, and $L(\omega)$ calculated in this way for Cd and Zn are plotted in Figs. 5a and 5b, respectively. It is clear from Fig. 5a that the loss function of Cd represents a fairly narrow peak at $E_p=8.98$ eV with a width $\Delta E_{1/2}=0.62$ eV, in very good agreement with the experimental results. In the case of Zn the agreement between the calculated loss function and the observed spectrum could be better. Possible reasons for the discrepancy will be discussed at the end of the present section, whereas now we shall turn to a more detailed discussion of Cd.

A microscopic calculation allowing for the contribution of the $4d$ electrons to the polarization gives practically the same width $\Delta E_{1/2}$ of the plasma resonance of Cd as the perturbation-theory calculation using the pseudopotential. However, the renormalization of the energy of plasma oscillations in accordance with the microscopic theory is greater and amounts to 2.3 eV. The reason for such a large shift can be understood if we write down, using Eqs. (10) and (14), the expression for Re $\varepsilon(\omega)$ separating deliberately the contributions from ranges of the energy below the interband transition E_d and above it:

$$\varepsilon_1(\omega)=1-\frac{\omega_p^2}{\omega^2}+\frac{2}{\pi}\int_0^{E_d} d\omega'\frac{\omega'\varepsilon_2(\omega')}{\omega'^2-\omega^2}+\frac{2}{\pi}\int_{E_d}^\infty d\omega'\frac{\omega'\varepsilon_2(\omega')}{\omega'^2-\omega^2}. \qquad (15)$$

It is clear from Fig. 5a that in the range of energies up to 10 eV the quantity $\varepsilon_2(\omega)$ assumes larger values at low ω, so that at the energy $\hbar\omega\approx9$ eV, i.e., near the plasma resonance, the denominator of the third term in Eq. (15) can be simplified by dropping the quantity ω'^2 compared with ω^2. Therefore, at $\hbar\omega\approx E_p$, we have approximately

$$\varepsilon_1(\omega)\approx1-\frac{\overset{\approx}{\omega}_p^2}{\omega^2}+\frac{2}{\pi}\int_{E_d}^\infty d\omega'\frac{\omega'\varepsilon_2(\omega')}{\omega'^2-\omega^2}, \qquad (16)$$

where

$$\overset{\approx}{\omega}_p^2=\tilde\omega_p^2+\frac{2}{\pi}\int_0^{E_d}d\omega'\omega'\varepsilon_2(\omega'). \qquad (17)$$

A direct calculation shows that Eq. (17) is approximately equal to ω_p^2, i.e., to the square of the frequency of classical plasma oscillations of the s electrons in Cd. This means that in the absence of the influence of the d electrons the plasma oscillations in Cd would have been of the same nature as in any other simple metal. The effect of the d electron polarization is contained in the last term of Eq. (16) and the calculated value of this term at $\hbar\omega\approx9$ eV is 0.58. It then follows trivially from Eq. (16) that because of the d-electron polarization the energy of plasma oscillations in Cd is renormalized to the value $\hbar\omega_p/\sqrt{1.58}\approx9$ eV. This means that the plasma-frequency shift in Cd is mainly due to the influence of the d-electron polarization and not due to the effects of the weak crystal potential in the conduction band.

In the case of Zn the present precision of the theoretical calculations of its dielectric properties is clearly insufficient for a correct reproduction of the experimental CEL spectra. First of all, as already pointed out in Ref. 28, the variational nature of the solution of the Schrödinger equation in the LMTO method gives for electrons less accurate wave functions than energies. This gives rise to errors in the determination of the matrix elements of the transitions and, consequently, to errors in $\varepsilon_2(\omega)$. These errors are less important for Cd, in which case—as demonstrated above—only certain integral characteristics of $\varepsilon_2(\omega)$ are important. However, in

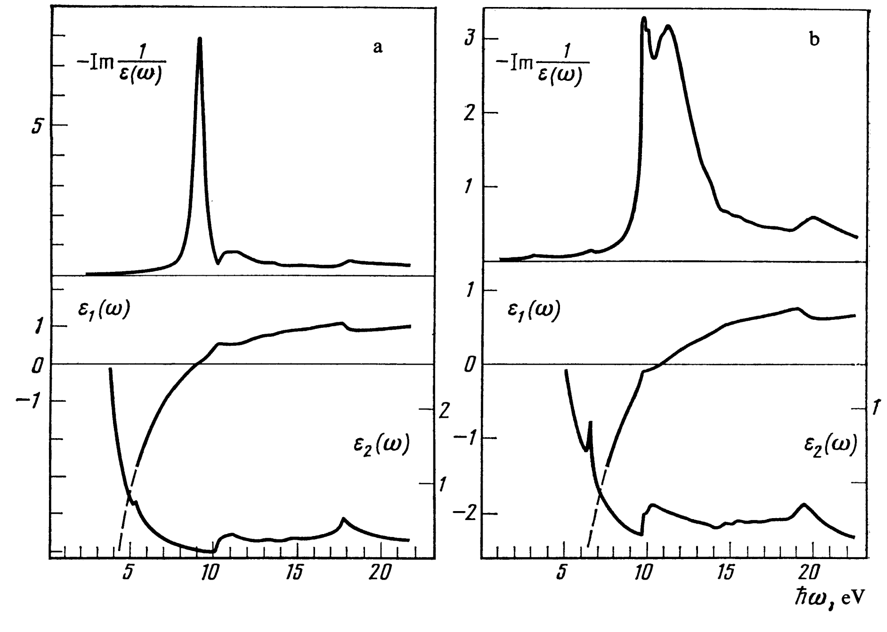

FIG. 5. Results of a microscopic calculation of the quantities $\varepsilon_1(\omega)$, $\varepsilon_2(\omega)$, and Im[− 1/ $\varepsilon(\omega)$] in the case of Cd (a) and Zn (b).

the case of Zn the precision in the determination of $\varepsilon_2(\omega)$ becomes very important already at energies in the interband-resonance region. Moreover, our calculations of the loss function ignore the local-field effect, which again may have its negative consequences in the delicate situation that is encountered in Zn. In this connection it would be very interesting to consider the experimental data on the optical absorption in Zn in a wide range of frequencies. When such data are available, it will become possible to compare directly the calculated and experimental $\varepsilon_2(\omega)$ curves and thus draw some conclusions on the accuracy of the calculations of the matrix elements of the transitions and of the functions $\varepsilon_2(\omega)$ as a whole.

4. CONCLUSIONS

We shall now formulate briefly the main results of our investigation and the problems that require further study. First of all, we obtained clear experimental data on the characteristic energy losses (CEL) experienced by fast (30 keV) electrons that penetrate right through thin Zn and Cd metal films. The corresponding CEL spectra are strikingly different for these two metals. Our theoretical analysis shows that in the range of excitation energies corresponding to plasma oscillations of electrons neither investigated substance can be regarded as an ordinary simple metal. In this range of energies the filled narrow *d* bands play an important role in Zn and Cd. In the case of Cd the 4*d* band is located below the Fermi level, the separation is greater than the energy of plasma excitation of the *s* electrons, and a plasma loss peak is very pronounced. However, this peak is shifted considerably in the direction of lower (compared with $\hbar\omega_p$) energies because of the 4*d*-electron polarization. In Zn, however, the 3*d* band is separated from the Fermi level by a gap less than $\hbar\omega_p$ so that the energy of the plasma excitation of the *s* electrons lies in the range of intensive interband transitions and the plasma resonance acquires a complex spectral distribution. However, plasmons of the kind observed in ordinary simple metals (i.e., quasimonochromatic weakly damped collective oscillations of the electron density) do not exist in Zn at all. It would be of considerable interest to investigate experimentally several other metals (for example In and Hg) which may manifest similar effects. We are still facing the problem of a more satisfactory theoretical description of the experimental data for Zn, for which we need a more accurate calculation of the energy band structure and of the dielectric function.

The authors are grateful to L. A. Elesin for electron-diffraction analysis and photomicrographs of the samples, and to Yu. A. Uspenskiĭ and I. I. Mazin for a valuable discussion of the results.

[1] N. W. Ashcroft and N. D. Mermin, Solid State Physics, Holt, Rinehart, and Winston, New York, 1976 (Russ. Transl., Mir, M., 1979).
[2] K. Sturm, Adv. Phys. **31**, 1 (1982).
[3] C. J. Powell, Proc. Phys. Soc. London **76**, 593 (1960).
[4] J. L. Robins, Proc. Phys. Soc. London **78**, 1177 (1961).
[5] R. J. Herickhoff, E. T. Arakawa, and R. D. Birkhoff, Phys. Rev. **137**, A1433 (1965).
[6] L. P. Mosteller Jr. and F. Wooten, Phys. Rev. **171**, 743 (1968).
[7] B. Feuerbacher and B. Fitton, Phys. Rev. Lett. **24**, 499 (1970).
[8] T. Aiyama and K. Yada, J. Phys. Soc. Jpn. **38**, 1357 (1975).
[9] H. Raether, Excitation of Plasmons and Interband Transitions by Electrons, Springer Verlag, Berlin, 1980 [Springer Tracts in Modern Physics, Vol. 88], pp. 50–51.
[10] R. T. Poole, P. C. Kemeny, J. Liesegang, J. G. Jenkin, and R. C. G. Leckey, J. Phys. F **3**, L46 (1973).
[11] R. A. Pollak, S. Kowalczyk, L. Ley, and D. A. Shirley, Phys. Rev. Lett. **29**, 274 (1972).
[12] S. Süzer, S. T. Lee, and D. A. Shirley, Phys. Rev. A **13**, 1842 (1976).
[13] F. J. Himpsel, D. E. Eastman, E. E. Koch, and A. R. Williams, Phys. Rev. B **22**, 4604 (1980).
[14] G. E. Juras, B. Segall, and C. B. Sommers, Solid State Commun. **10**, 427 (1972).
[15] V. L. Moruzzi, J. F. Janak, and A. R. Williams, Calculated Electronic Properties of Metals, Pergamon Press, Oxford, 1978.
[16] K. A. Moldosanov and M. V. Zharnikov, Prib. Tekh. Eksp. No. 2, 25 (1984).

[17] V.D. Gorobchenko, M. V. Zharnikov, E. G. Maksimov, and K. A. Moldosanov, Zh. Eksp. Teor. Fiz. **86**, 597 (1984) [Sov. Phys. JETP **59**, 348 (1984)].
[18] R. L. Hengehold and F. L. Pedrotti, J. Appl. Phys. **47**, 287 (1976).
[19] D. E. Bradley, in: Techniques for Electron Microscopy (ed. by D. H. Kay), 2nd ed., Blackwell, Oxford, 1965, pp. 58–74.
[20] V. D. Gorobchenko and E. G. Maksimov, Usp. Fiz. Nauk **130**, 65 (1980) [Sov. Phys. Usp. **23**, 35 (1980)].
[21] V. D. Gorobchenko and E. G. Maksimov, Zh. Eksp. Teor. Fiz. **81**, 1847 (1981) [Sov. Phys. JETP **54**, 978 (1981)].
[22] S. L. Adler, Phys. Rev. **126**, 413 (1962).
[23] G. M. Gandel'man and V. M. Ermachenko, Zh. Eksp. Teor. Fiz. **45**, 522 (1963) [Sov. Phys. JETP **18**, 358 (1964)].
[24] N. Wiser, Phys. Rev. **129**, 62 (1963).
[25] Yu. Kagan, V. V. Pushkarev, and A. Holas, Zh. Eksp. Teor. Fiz. **84**, 1494 (1983) [Sov. Phys. JETP **57**, 870 (1983)].
[26] H. Ehrenreich and M. H. Cohen, Phys. Rev. **115**, 786 (1959).
[27] O. K. Andersen, Phys. Rev. B **12**, 3060 (1975).
[28] Yu. A. Uspenski, E. G. Maksimov, S. N. Rashkeev, and I. I. Mazin, Z. Phys. B **53**, 263 (1983).

Translated by A. Tybulewicz